Isomerization of 1-Butene on Silica-Alumina: Kinetic Modeling and Catalyst Deactivation

F. Garcia-Ochoa and A. Santos
Dept. de Ingeniería Química, Universidad Complutense, Madrid, Spain

In the study of 1-butene isomerization on a silica-alumina catalyst 448–523 K, cis-2-butene and trans-2-butene are detected. Based on BSTR experimental data and zero-time prediction kinetic models using the Langmuir-Hinshelwood mechanism are assumed to develop kinetic equations for which a triangular reaction scheme is used. In four different mechanisms, one and two active sites take part in the surface reaction as the controlling step and then the deactivation rate determined considering two types of experimental data from BSTR and by measuring weight changes of a catalyst particle from coke deposition in an electrobalance. A coke precursor is assumed formed by reaction of adsorbed molecules (of any butene isomer) and gas-phase molecules. Activity- and coke-content-time data allow us to choose a model whose activation energies of the deactivation kinetic parameter are closer in value. Coke is assumed deposited in a monolayer. The model chosen shows a triangular scheme, kinetic equations of the reaction for fresh catalyst with two active sites in the surface reaction, and the deactivation rate according to a coke formation mechanism in which a precursor is formed by reaction of 3 adsorbed molecules and 1 molecule in the gas phase. It accurately fits both BSTR conversion-time data and electrobalance coke-content data. The coke formation mechanism establishes relationships of activity vs. coke content and catalyst acidity which are supported by experimental results.

Introduction

1-Butene isomerization has been widely studied, using three types of catalysts: *basic catalysts* (Haag and Pines, 1960a), *acid catalysts* (Foster and Cetanovic, 1960; Haag and Pines, 1960b; Hightower and Hall, 1967; Hightower et al., 1967; Ghorbel et al., 1973, 1974; Medema, 1975; Vinek et al., 1975; Aguayo et al., 1990), and *supported metals catalysts* (Carrá and Ragaini, 1968; Chang et al., 1973; Rosynek and Fox, 1977; Goldwasser et al., 1981; Ragaini and Cattania-Sabbadini, 1985; Eliyas et al., 1987). In these studies the focus has been in the reaction scheme determination, because this reaction has been taken as representative of olefine isomerization, where the product distribution is of great interest (Medema, 1975). The more general reaction scheme, valid for the three different catalyst types is:

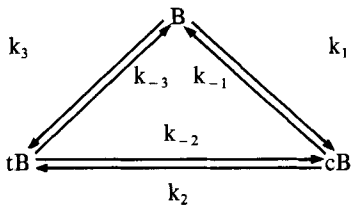

(1)

the production rates of different isomers can be written as:

$$R_{cB} = r_1 - r_2$$
$$R_{tB} = r_2 + r_3$$
$$-R_B = r_1 + r_3 \qquad (2)$$

The kinetic equations for the three reactions in the scheme of Eq. 1 have usually been considered as power-law (Foster and Cvetanovic, 1960; Haag and Pines, 1960a,b; Hightower and Hall, 1967; Hightower et al., 1967; Chang et al., 1973; Vinek et al., 1985); hyperbolic models have been considered recently (Ragaini and Cattania-Sabbadini, 1985; Eliyas et al., 1987; Aguayo et al., 1990), and only one mechanism (supposing all the butene isomers to be adsorbed in one active site) is taken into account to obtain LHHW (Langmuir-Hinselwood-Hougen-Watson) models.

The possible catalyst deactivation by coking and the possible effect on catalyst selectivity (Ballivet et al., 1970) are infrequently considered in literature. Considering that, when acid catalysts are employed, coke formation is unavoidable and catalyst activity decays and selectivity changes. The correct description of the system evolution must take into account the change of catalyst activity.

Catalyst deactivation by coking has been considered in the literature with activity-time relationships (Chu, 1968; Levenspiel, 1972; Jodra et al., 1976) and using coke deposited-time relationships (De Paw and Froment, 1975; Dumez and Froment, 1976; Lin et al., 1983; Froment and Bischoff, 1990). Only a small number of articles theoretically try to establish a relationship between both approaches (Nam and Kittrell, 1984).

In this article, 1-butene isomerization on a silica-alumina catalyst is studied, and the kinetic model of the main reaction (including both a reaction scheme and kinetic equations for each one of the reactions taking part) is determined. Several LHHW models are taken into account for the kinetic equations of the reactions. The deactivation rate is also determined, using both activity-time data and coke content-time data. The main objective of this work is the coupling of the reaction mechanism with the coke formation mechanism. The relationships between both deactivation rate and coke deposition rate, and between activity and coke content will be established. It will also be shown that the combination of the kinetic and coking data can be used by kinetic model discrimination, always taking into account a possible mechanism for the main reaction and for coke formation.

Theoretical

According to the network of reactions given in Eq. 1, different catalyst activities can be defined, one for each of the reactions of the scheme:

$$r_i = r_{io} \cdot \alpha_i \quad i = 1, 2, 3 \tag{3}$$

Catalyst deactivation rate can be described according to the following equation (Jodra et al., 1976):

$$r_{d_i} = -\frac{d\alpha_i}{dt} = \psi_i(T, P) \cdot \alpha_i^d \quad i = 1, 2, 3 \tag{4}$$

where $\psi_i(T, P)$ is a function of temperature and composition.

The deactivation rate can be described by a kinetic equation for coke formation (Dumez and Froment, 1976):

$$r_c = \frac{dC_c}{dt} = \varphi(T, P) \cdot \alpha_c \tag{5}$$

where $\varphi(T, P)$ is also a function of temperature and composition, and α_c is the catalyst activity for the coke formation reaction, given by the following equation (Dumez and Froment, 1976; Lin et al., 1983):

$$\alpha_c = \phi(C_c) \tag{6}$$

where $\phi(C_c)$ is a function of the coke content.

To obtain relationships between r_d and r_c, and between α_i and α_c, it is necessary to suppose a coke formation mechanism. It is usually accepted that coke is a polymer formed from a precursor, P_{S_h}, which is in turn produced from both reacting compounds adsorbed and gas-phase molecules. Active site coverage, coke formation, and pore blockage are due to such a precursor. In the 1-butene isomerization, the coke precursor can be formed from all three isomers, 1-butene, cis- and trans-2-butene. The following mechanisms are proposed for coke precursor formation (Santos, 1992):

$$\begin{aligned}
&B + m_{1B}s \rightarrow m_{1B}B_{1/m_{1B}}s \\
&cB + m_{2B}s \rightarrow m_{2B}cB_{1/m_{2B}}s \\
&tB + m_{2B}s \rightarrow m_{2B}tB_{1/m_{2B}}s \\
&nB(g) + hB_{1/m_{1B}}s \rightarrow Ps_h \\
&ncB(g) + hcB_{1/m_{2B}}s \rightarrow Ps_h \\
&ntB(g) + htB_{1/m_{2B}}s \rightarrow Ps_h
\end{aligned} \tag{7}$$

where m_{1B}, m_{2B} are the number of active sites involved in the surface adsorption step for 1-butene and 2-butenes, respectively; h and n are the number of adsorbed butene molecules and the number of molecules in gaseous phase, respectively, reacting to produce the coke precursor.

The activity for the different reactions, α_i, can be deduced from Eq. 7. The activity follows a power-law dependence with the ratio between the number of active sites at a time and the number of active sites in the fresh catalyst (Nam and Kittrell, 1984; Froment and Bischoff, 1990). Using the coke precursor concentration, C_{PSh}, it can be calculated from the following relation:

$$\alpha_i = \left(\frac{S_o - S_p}{S_o}\right)^{m_i} = \left(\frac{S_o - h \cdot C_{Ps_h}}{S_o}\right)^{m_i} \tag{8}$$

where m_i is the number of active sites taking part in the controlling step of the reaction i. From Eq. 8 the following relationship between catalyst activity for two reactions, i and j, can be written as:

$$\alpha_i = \alpha_j^{m_i/m_j} \tag{9}$$

Therefore, when the number of active sites involved in the different reactions is the same, the catalyst activity is also the same for the different reactions, and this is the most probable case in the 1-butene isomerization. In this case, it is possible to employ only one deactivation rate r_d that, from Eq. 8, is related with the coke precursor formation rate as follows:

$$\frac{-d\alpha}{dt} = \frac{h \cdot m}{S_o} \cdot \alpha^{m-1/m} \cdot \frac{dC_{Ps_h}}{dt} \tag{10}$$

According to the mechanism of coke precursor formation given by Eq. 7, the production rate of that precursor can be written as:

$$\frac{dC_{Ps_h}}{dt}=\frac{kd'_B\cdot K_B^{h/m_{1B}}\cdot P_B^{(h/m_{1B})+n}+kd'_{2B}\cdot K_{2B}^{h/m_{2B}}\cdot (P_{cB}^{(h/m_{2B})+n}+P_{tB}^{(h/m_{2B})+n})}{[1+(K_B\cdot P_B)^{1/m_{1B}}+K_{2B}^{1/m_{2B}}\cdot (P_{cB}^{1/m_{2B}}+P_{tB}^{1/m_{2B}})]^h}\cdot (S_o-S_p)^h \quad (11)$$

and taking into account Eqs. 8, 10, and 11, the deactivation rate can be written as:

$$-\frac{d\alpha}{dt}=\frac{kd_B\cdot K_B^{h/m_{1B}}\cdot P_B^{(h/m_{1B})+n}+kd_{2B}\cdot K_{2B}^{h/m_{2B}}\cdot (P_{cB}^{(h/m_{2B})+n}+P_{tB}^{(h/m_{2B})+n})}{[1+(K_B\cdot P_B)^{1/m_{1B}}+K_{2B}^{1/m_{2B}}\cdot (P_{cB}^{1/m_{2B}}+P_{tB}^{1/m_{2B}})]^h}\cdot \alpha^{(m+h-1)/m} \quad (12)$$

From Eqs. 12 and 4 the following equations can be obtained:

$$\psi(T,P)=\frac{kd_B\cdot K_B^{h/m_{1B}}\cdot P_B^{(h/m_{1B})+n}+kd_{2B}\cdot K_{2B}^{h/m_{2B}}\cdot (P_{cB}^{(h/m_{2B})+n}+P_{tB}^{(h/m_{2B})+n})}{[1+(K_B\cdot P_B)^{1/m_{1B}}+K_{2B}^{1/m_{2B}}\cdot (P_{cB}^{1/m_{2B}}+P_{tB}^{1/m_{2B}})]^h} \quad (13)$$

$$d=\frac{m+h-1}{m} \quad (14)$$

When the coke content is small, such as, under 6% (w/w) in silica-alumina catalysts, it can be assumed that a monolayer of coke is deposited on the catalyst surface (Acharya et al., 1990). According to Nam and Kittrell (1984), the following linear relationship can be assumed between the precursor and the coke concentrations:

$$C_c=C_{cm}=C_{Ps_h}\cdot M_c \quad (15)$$

If Eqs. 8 and 15 are combined, the catalyst activity and coke content relationship can be written as (Nam and Kittrell, 1984):

$$C_c=\frac{S_o\cdot M_c}{h}\cdot (1-\alpha^{1/m}) \quad (16)$$

Differentiation of Eq. 16 provides the coke production rate:

$$\frac{dC_c}{dt}=\frac{S_o\cdot M_c}{h\cdot m}\cdot \psi(T,P)\cdot \alpha^{h/m} \quad (17)$$

From the comparison between Eq. 5 and Eq. 17, the following relationships can be deduced:

$$\alpha_c=\alpha^{h/m} \quad (18)$$

$$\varphi(T,P)=\frac{S_o\cdot M_c}{h}\cdot \psi(T,P) \quad (19)$$

where the function $\psi(T,P)$ in Eq. 17 is the same as in Eq. 4 in which the 1-butene isomerization can be established according to Eqs. 13 and 14.

When the experimental data are obtained in differential conditions, that is, for small changes in the gas-phase composition, the function $\psi(T,P)$ can be assumed to remain constant. Then Eq. 4 can be integrated to provide (Jodra et al., 1976):

$$\alpha=\exp[-\psi(T,P)\cdot t] \because d=1 \quad (20)$$

$$\alpha=\left[\frac{1}{1+(d-1)\cdot\psi(T,P)\cdot t}\right]^{1/d-1} \because d\neq 1 \quad (21)$$

as order d can be expressed as a function of h and m (Eqs. 13 and 14), it is possible by substituting of Eqs. 20 or 21 into Eq. 17 to obtain the following integrated equations, depending on the h value:

$$h=1 \therefore C_c=\frac{S_o\cdot M_c}{h}\cdot\left[1-\exp\left(\frac{-\psi(T,P)\cdot t}{m}\right)\right] \quad (22)$$

$$h\neq 1 \therefore C_c=\frac{S_o\cdot M_c}{h}\cdot\left\{1-\left[1+\frac{h-1}{m}\cdot\psi(T,P)\cdot t\right]^{1/1-h}\right\} \quad (23)$$

Therefore, the type and parameters of function $\psi(T,P)$ can be obtained by interpretation of activity-time data or of coke content-time data. The function and parameter values must be the same at least for one of the possible models, which is capable of connecting the two different approaches described above.

Experimental Studies

Isomerization of 1-butene has been studied in two experimental setups:

(a) A basket catalytic reactor (BSTR) was used to carry out experiments at different temperatures and space times. The outlet gas stream was analyzed by gas-liquid chromatography, obtaining 1-butene, 2-cis- and 2-trans-butene conversion variation with time. From these data both conversion at zero time, by extrapolation, and activity were obtained.

(b) An electrobalance was employed to determine the coke

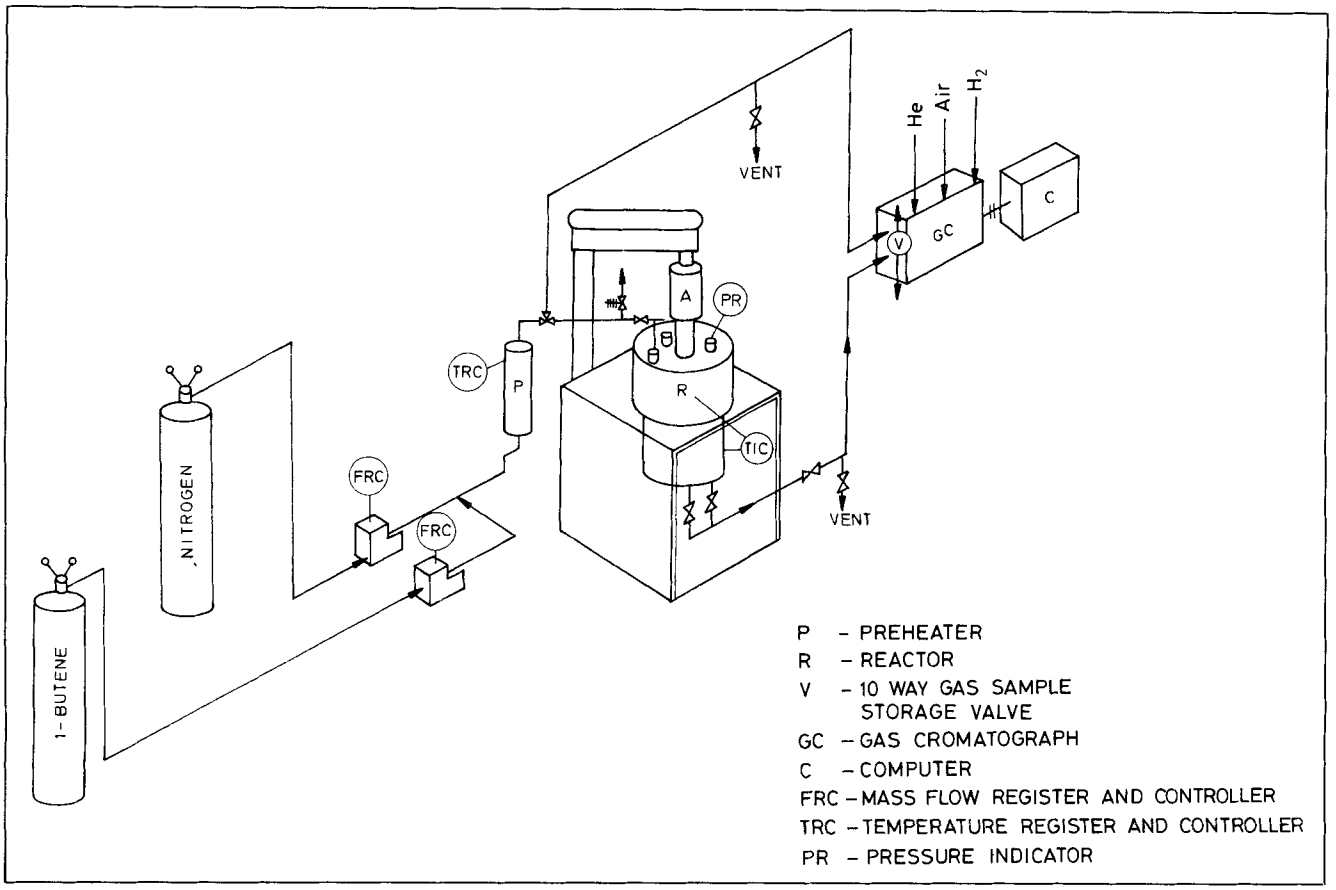

Figure 1. BSTR installation.

formation rate. In these experiments the weight increase of catalyst powder due to coke formation was measured in the same interval of temperature and composition as those employed in the above mentioned setup.

1-Butene isomerization and coke deposition were studied between 448 and 523 K, using inlet 1-butene partial pressures, ranging from 0.2 to 1.02 atm.

Figure 1 shows the BSTR installation. BSTR was a 500-cm^3 stainless steel vessel from Autoclave Engineers. The basket was filled with catalyst particles, and then a nitrogen stream was fed until the required temperature was reached, followed by feeding 1-butene. Steady-state was achieved in 5 or 10 min due to the use of stirrer speed controllers, mass-flow controllers, and temperature controllers in several parts of the installation. Gas stream from the reactor was automatically injected to an on-line gas-liquid chromatograph (Hewlett-Packard 5890 series II) at time intervals between 5 and 50 min. The experiment was ended between 24 and 48 h later by passing pure nitrogen until hydrocarbons were not detected by the analysis mentioned before, approximately 10 or 20 min later. The system was then cooled, and the catalyst was withdrawn from the basket for coke content and properties determination.

The gas stream analysis was performed by G-L chromatography using a FI detector and a column of picric acid 0.9% on Graphpac-GC 80/100 mesh 2.3 m in length and 1/8 in. in dia. Oven temperature was controlled at 30°C, and helium was used as carrier, at 22 cm^3/min. In this way 1-butene, 2-cis-butene and 2-trans-butene were the peaks detected in all the experiments. Only in some cases was isobutene formed, always under 0.5%.

The electrobalance shown in Figure 2 is formed by a gas feed system, with three mass-flow controllers, the balance MK-2 Vacuum Head from Electronic Ltd., and a data acquisition system able to detect a weight variation of 1 μg. In each experiment, around 200 mg of fresh catalyst was placed inside a basket assuming a good contact between gas and solid. First, nitrogen was fed and the system was heated until a fixed temperature was reached. That temperature was measured by a thermocouple located very close to that basket less than 0.5 cm away. Then a gaseous stream with 1-butene and nitrogen was fed, and the weight change data was collected. Once the experiment was finished, the catalyst was recovered for coke content and properties analysis.

1-Butene 99.3% in purity (liquid carbonic) and nitrogen 99.998% in purity (liquid carbonic) as inert were used. The impurities of 1-butene were mainly 2-butenes and isobutene.

A commercial silica-alumina catalyst from Südchemie (KA-3) was used. Specific surface was determined by B.E.T. (Brunauer, Emmett, Teller) method using a Micromeritics Accusorb 2000 Sorptometer. Pore-size distribution (macro and microporosity) was measured using a mercury porosimeter Carlo Erba Milestone 2000 and a Coulter Omnisorb 100 Sorptometer. Coke analysis was performed by elemental analysis with a Leco HCM 600. N-butilamine (Carlo Erba) 99% diluted

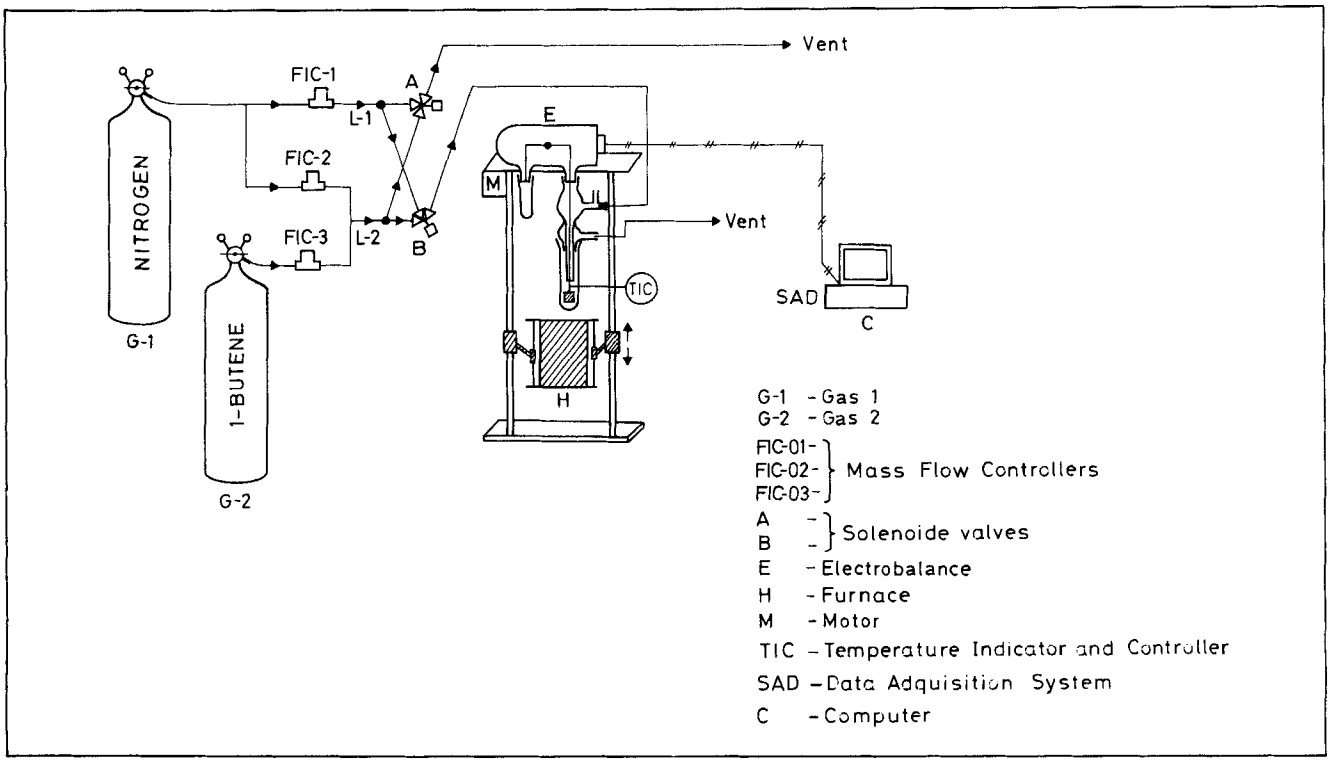

Figure 2. Electrobalance.

in benzene (dry, from Merck) was used for catalyst acidity measurements. The fresh catalyst has the following values: S_g(B.E.T) = 126 m^2/g and $V_p = 0.587$ cm^3/g.

Experimental results in BSTR

Three different groups of experiments were carried out in this reactor. In all of them a stirrer speed of 1,000 rpm and a catalyst particle diameter of 0.1 cm were used. At the maximum temperature employed these conditions were experimentally checked with no diffusional limitations being found by either interphase (over 800 rpm) and intraphase (particle diameter under 0.15 cm) transfer processes (Santos, 1992). The three groups of experiments are as follows:

Group I: 18 runs were carried out by changing temperature (448 and 523 K) and space time (between 0.907 and 55.921 g·h/mol), maintaining the feed composition constant, a partial pressure of 1-butene of 0.74 atm.

Group II: Another 28 runs were carried out by changing temperature (448, 473, 498 and 523 K), space time (between 0.244 and 2.158 g·h/mol), and feed composition (P_{Bo} between 0.20 and 0.89 atm) trying to maintain the reactor in differential operation, that is, with a small change between inlet and outlet composition under 0.10 of 1-butene conversion in most of the runs. In some runs it was slightly higher, with a maximum value of 0.131.

Group III: In this group 25 runs were carried out at three temperatures (473, 498, and 523 K), different space time (between 1.363 and 48.77 g·h/mol) and feed composition (P_{Bo} between 0.31 and 1.02 atm) with a high conversion of 1-butene (until 0.703 at zero time) following the variation of the conversion with time to study the catalyst deactivation.

The results obtained in these three groups of experiments are shown in Tables 1, 2, and 3 corresponding to Groups I, II, and III for the latter only at zero time, that is, for fresh catalyst. In these tables conversion of 1-butene, X_B, is shown; however, conversion to 2-cis-butene, X_{cB}, and to 2-trans-butene, X_{tB}, were measured. The reaction has two key components, any two of the three butene isomers detected. As one

Table 1. Conversion and Selectivity of Group I Experiments at Constant Inlet 1-Butene Partial Pressure (P_{Bo} = 0.74 atm)

Run	W/F_{Bo}	X_B	S_c
	$T = 448$ K		
1	0.907	0.074	1.056
2	1.037	0.097	1.088
3	1.454	0.120	1.075
4	2.460	0.185	1.022
5	3.014	0.224	1.009
6	3.539	0.242	1.000
7	4.225	0.267	0.992
8	5.270	0.300	0.973
9	7.052	0.348	0.949
10	10.550	0.424	0.893
11	13.970	0.515	0.780
12	27.960	0.641	0.659
13	55.921	0.730	0.617
	$T = 523$ K		
14	1.666	0.268	0.846
15	2.082	0.307	0.808
16	2.777	0.375	0.830
17	4.165	0.447	0.795
18	8.329	0.557	0.762

Table 2. Conversion and Selectivity of Group II Experiments in Differential Reactor

Run	W/F_{Bo}	P_{Bo}	X_B	S_c
		$T=448\ K$		
19	2.158	0.20	0.089	1.045
20	1.439	0.28	0.081	1.057
21	1.071	0.41	0.074	1.074
22	0.864	0.53	0.071	1.074
23	0.864	0.61	0.082	1.072
24	0.720	0.78	0.070	1.102
25	0.540	0.89	0.054	1.073
		$T=473\ K$		
26	1.934	0.20	0.101	1.006
27	1.290	0.28	0.092	0.998
28	0.967	0.41	0.088	0.989
29	0.775	0.53	0.089	1.002
30	0.773	0.61	0.101	0.984
31	0.645	0.78	0.095	0.968
32	0.483	0.89	0.079	0.982
		$T=498\ K$		
33	1.792	0.20	0.123	1.054
34	1.195	0.28	0.112	1.043
35	0.896	0.41	0.115	0.995
36	0.717	0.53	0.119	1.042
37	0.717	0.61	0.129	1.047
38	0.597	0.78	0.131	1.029
39	0.448	0.89	0.114	1.018
		$T=523\ K$		
40	0.977	0.20	0.102	1.077
41	0.652	0.28	0.091	0.999
42	0.487	0.41	0.100	1.073
43	0.391	0.53	0.106	1.078
44	0.391	0.61	0.114	1.080
45	0.326	0.78	0.111	1.059
46	0.244	0.89	0.094	1.042

more component was measured, experimental error was calculated and found to be very low, always under 10% and often around 5%. Also selectivity to 2-cis-butene, S_c, is shown in these tables, calculated as:

$$S_c = \frac{R_{cB}}{R_{tB}} = \frac{X_{cB}}{X_{tB}} \tag{24}$$

Table 3. Initial Conversion and Selectivity of Group III Experiments for Space Time and 1-Butene Partial Pressure

Run	W/F_{Bo}	P_{Bo}	X_B	S_c
		$T=473\ (K)$		
47	2.290	0.92	0.304	0.883
48	5.928	0.87	0.485	0.660
49	4.930	0.74	0.389	0.793
50	1.071	0.61	0.125	1.024
51	2.324	0.41	0.222	0.984
52	14.19	0.41	0.500	0.758
53	24.14	0.41	0.569	0.735
54	48.77	0.40	0.703	0.661
55	5.350	0.34	0.336	0.906
56	24.14	0.34	0.516	0.748
		$T=498\ K$		
57	6.168	0.86	0.517	0.615
58	9.457	0.74	0.555	0.647
59	2.715	0.67	0.320	0.869
60	14.18	0.62	0.606	0.650
61	21.49	0.58	0.667	0.631
62	3.024	0.49	0.281	0.876
63	5.620	0.36	0.367	0.784
64	12.23	0.31	0.500	0.756
		$T=523\ K$		
65	1.363	1.02	0.317	0.774
66	1.704	0.98	0.342	0.770
67	1.765	0.86	0.329	0.780
68	1.769	0.78	0.309	0.792
69	1.371	0.74	0.251	0.788
70	1.720	0.62	0.273	0.824
71	2.952	0.37	0.312	0.818

In some of the experiments of Group III the catalyst was recovered when the run was finished and the coke content, the coke elemental composition, the acidity, the surface, and the pore volume were determined for catalyst with different activities. These results are given in Table 4.

Experimental results in electrobalance

Another group of experiments was carried out in the electrobalance setup described in Figure 2, where the weight change of the catalyst powder was measured with time on-stream.

Table 4. Physical Properties, Acidity and Coke Content for Fresh and Aged Catalyst

Run	$T(K)$	α	S_g m^2/g	V_p cm^3/g	A meq/g	% C_c (g/g) Total	C	H
Fresh Catalyst	--	1	126	0.587	9.5	0	0	0
47	473	0.46	121	0.579	5.5	0.8	0.4	0.4
49	473	0.7	123	0.592	7.3	0.6	0.3	0.3
52	473	0.61	127	0.569	7.3	0.6	0.3	0.3
62	498	0.64	125	0.569	7.7	0.6	0.3	0.3
62a	498	0.73	130	0.581	7.7	0.3	0.1	0.2
62b	498	0.66	118	0.582	7.3	0.5	0.3	0.2
62c	498	0.5	122	0.578	5.5	0.7	0.4	0.3
62d	498	0.4	123	0.573	6.2	0.8	0.5	0.3
63	498	0.56	115	0.581	6.6	0.5	0.3	0.2
64	498	0.81	129	0.578	8.5	0.3	0.1	0.2
70	523	0.3	119	0.565	5.4	0.9	0.5	0.4

Table 5. Conditions and Time of Data Acquisition of Group IV Experiments Electrobalance Runs

Run	W(mg)	$T(K)$	P_{Bo} (atm)	t (min)
1	200	473	0.2	5,000
2	200	473	0.41	5,000
3	200	473	0.74	2,000
4	200	498	0.41	3,000
5	200	498	0.6	6,000
6	200	498	0.86	3,000
7	200	523	0.41	3,000
8	200	523	0.6	3,000
9	200	523	0.86	3,000

Group IV: The experimental conditions of these runs are shown in Table 5; as can be seen nine runs were carried out at three temperatures (473, 498, and 523 K), changing the 1-butene partial pressure (between 0.2 and 0.86 atm), obtaining the weight increase of a sample of 200 mg of catalyst during a time between 2,000 and 6,000 min.

Kinetic Model of the Main Reaction

First, the discrimination among different reaction schemes was carried out using the results from Groups I and II of the experiments. Four possibilities were taken into account, that is, the general scheme given by Eq. 1 and the following three simplified schemes including two schemes considering two consecutive reactions and another one according to two parallel reactions:

$$B \underset{k_{-1}}{\overset{k_1}{\rightleftharpoons}} cB \underset{k_{-2}}{\overset{k_2}{\rightleftharpoons}} tB \tag{25}$$

$$B \underset{k_{-3}}{\overset{k^3}{\rightleftharpoons}} tB \underset{k_{-2}}{\overset{k^2}{\rightleftharpoons}} cB \tag{26}$$

$$cB \underset{k_1}{\overset{k^{-1}}{\rightleftharpoons}} B \underset{k_{-3}}{\overset{k^3}{\rightleftharpoons}} tB \tag{27}$$

The variation of X_B, X_{cB}, and X_{tB} with W/F_{Bo} in Group I of experiments is shown in Figure 3(A and B, for 448 and 523 K, respectively). From this Figure, it is evident that any of either cis- and trans-2-butene isomers is formed from the other at the beginning of the reaction, and any maximum in some of those concentrations is not observed. Therefore, the selectivity to 2-cis-butene, S_c, for $X_B \to 0$, has a value very close to 1, as can be seen in Figure 4. According to such a variation, both schemes including consecutive reactions corresponding to Eqs. 25 and 26 can be rejected. On the other side, Figure 5 shows how S_c decreases as X_B increases, that is, P_{cB} and P_{tB} increase. This cannot be explained with the parallel scheme of Eq. 27. Therefore, it is necessary to take into account the more complicated scheme corresponding to Eq. 1.

To obtain the kinetic model at zero time with fresh catalyst a thermodynamic study for equilibrium constant estimation of the three reactions in the triangular scheme of Eq. 1 was made, using the method described by Hougen et al. (1954) with data from Reid et al. (1977). The values obtained are given in Table 6 for the four temperatures studied. Following this, discriminating among different possibilities of kinetic equations for the three different reactions in Eq. 1, an initial reaction rates analysis was carried out using the data from Group II of experiments (Table 2). The production rates of the different compounds can be calculated as:

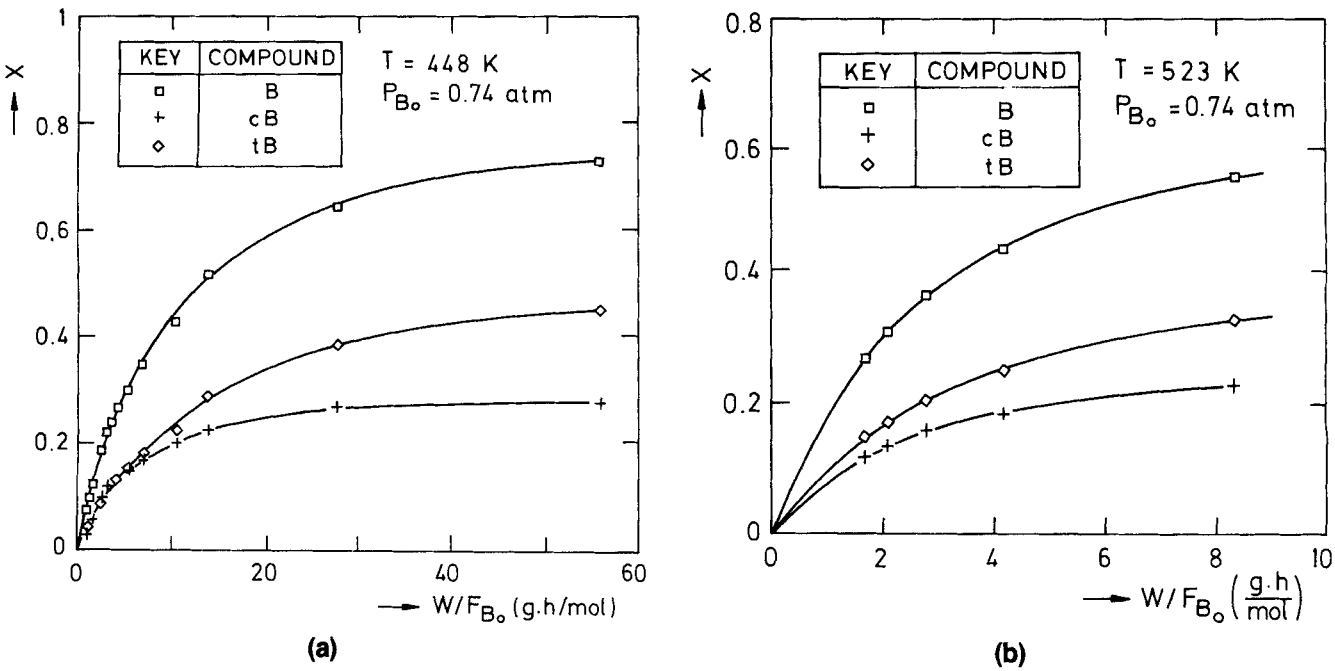

Figure 3. Influence of space time in 1-butene conversion employing constant inlet 1-butene partial pressure.
(a): 448 K; (b) 523 K.

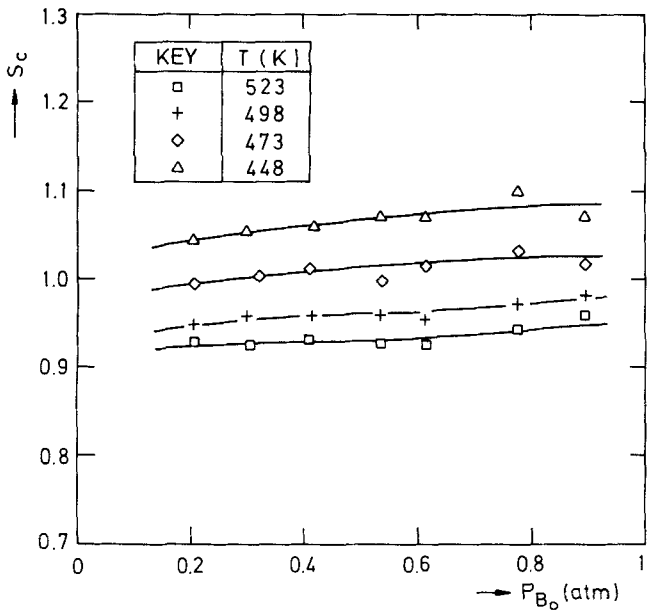

Figure 4. Variation of cis-2-butene selectivity with inlet 1-butene partial pressure.

Data from differential reactor.

$$R_k = \frac{X_k}{W/F_{Bo}} \quad k = B,\ cB,\ tB \tag{28}$$

If the variation of such production rates, R_k, with inlet 1-butene partial pressure, P_{Bo}, is analyzed (see Figure 6), it can be concluded that 1-butene adsorption is not the controlling step of the process rate. As shown in Figure 6, the 1-butene production rate does not follow a linear relationship with inlet 1-butene partial pressure. On the other hand, the desorption of only one 2-butene isomer is not the controlling step either, because there is not a consistent relationship between the partial pressure of the other 2-butene isomer and the partial pressure of 1-butene (such ratio would be given by the equilibrium). Finally, the desorption of both 2-butene cannot be the controlling step, because in such a case the 2-butene partial pressures, would not appear in the adsorption term of the kinetic model and this yielded a great residual in the fitting to experimental data. Thus, surface reaction was assumed to be the controlling step.

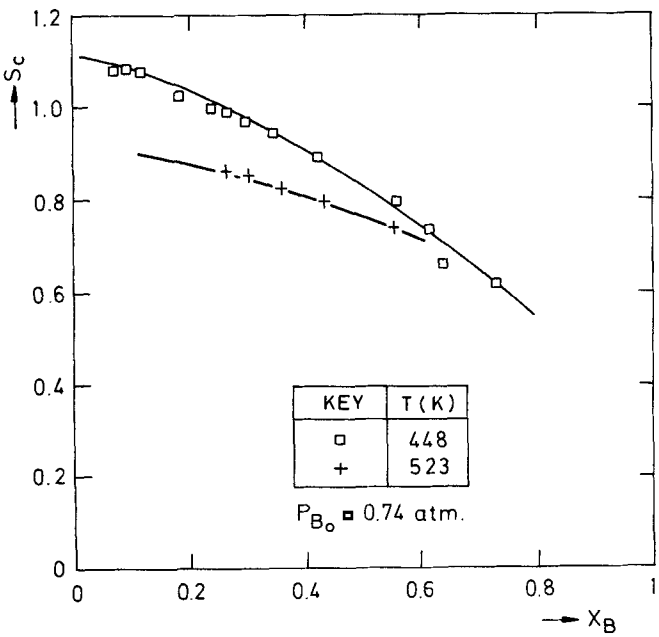

Figure 5. Variation of cis-2-butene selectivity with total 1-butene conversion for constant inlet 1-butene partial pressure.

Table 6. Equilibrium Constant Values for Reaction Scheme of Eq. 1

$T(K)$	K_{e1}	K_{e2}	K_{e3}
448	3.36	1.96	6.58
473	3.07	1.89	5.67
498	2.71	1.81	4.71
523	2.10	1.64	3.44

Four different mechanisms have been considered, as shown in Table 7, in which surface reaction is assumed to be the controlling step, and the kinetic equations given in the same table are obtained. The discrimination among models I-1 through I-4 has been attempted in different ways:

- Data from the differential reactor, those corresponding to Group II of experiments (Table 2) have been interpreted using only the production rate of 1-butene by linear regression (after linearization of the different models in Table 7) at each temperature, and by nonlinear regression (Marquardt, 1963) with the data achieved at all the temperatures. The four models in Table 7 yield parameter values and fit the statistical and physical criteria adopted (Garcia-Ochoa et al., 1989, 1990), and no discrimination among them is possible.
- Data from the integral reactor, corresponding to Groups I and III of experiments (Tables 1 and 3) have been interpreted by multiresponse nonlinear regression using cis-2-butene and trans-2-butene production rates as responses (two key compounds), both at each temperature and at all data with the temperature as variable. In this way the best results are reached if one of the parameters, $\Delta H_B/R$, is fixed in a previously calculated value. Thus, parameter $\Delta H_B/R$ of the adsorption equilibrium constant of 1-butene was calculated from experiments carried out in a chromatographic column filled with the same silica alumina used as catalyst (Santos, 1992). The values thus obtained are shown in Table 8, that is, a value of $-2{,}810$ K or a value of $-2{,}574$ K depending on whether one or two active sites are considered to be involved in the mechanism assumed.

In the last case, the four models of Table 7 provide very similar results: a very good fitting according to the square residual sum (SRC) and narrow intervals for all but one of the parameter values (for 95% of confidence), except for one of them. The thermodynamic criteria of Boudart et al. (1967) were also applied, and again all four models I-1 to I-4 fulfill such criteria. Therefore, the final discrimination of the kinetic model of the main reaction was carried out analyzing the rate of deactivation.

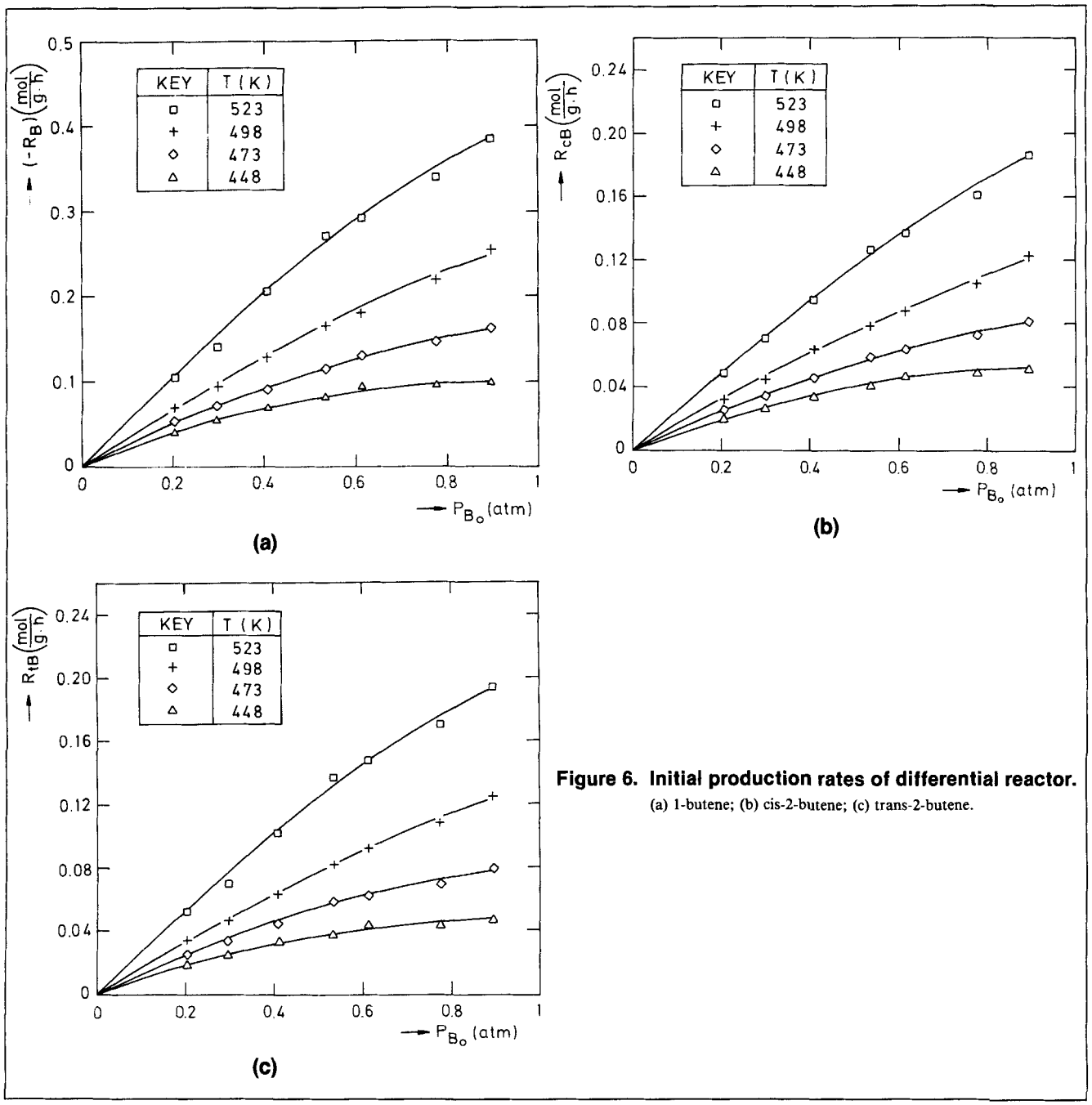

Figure 6. Initial production rates of differential reactor.
(a) 1-butene; (b) cis-2-butene; (c) trans-2-butene.

Deactivation Kinetic Model

Assuming the triangular scheme of Eq. 1 for the 1-butene isomerization, three reactions are taking place, each one with a different activity: α_1, α_2 and α_3, with the relationship among them given by Eq. 9. For each of the four mechanisms shown in Table 7, the value of m (number of active sites involved in the surface reaction step) is the same for all three reactions (m is 1 for mechanism of model I-1 and m is 2 for mechanisms of models I-2 to I-4). Therefore, the activities of the different reactions must be the same: $\alpha_1 = \alpha_2 = \alpha_3 = \alpha$, according to Eq. 9.

Thus, taking into account Eqs. 2 and 3, the activity α at any time can be calculated from Eq. 29, with both production rates at the same composition and temperature:

$$\alpha = \frac{R_k}{(R_k)_o} \quad k = B,\ cB,\ tB \tag{29}$$

For experimental checking of the assumption of a single activity value for the three reactions, Eq. 29 can be applied for each of the butene isomers. This has been done with the experimental data from Group III given in Table 3. Figure 7 is an example of some of the results obtained, where α has been calculated for the three isomers, B, cB, and tB, according to the following approach:

Table 7. Kinetic Models of Different Mechanisms and Kinetic Equations with Surface Reaction as Controlling Step

* = Controlling Step	Mechanism	Kinetic Equations
	Model I-1	
	$B+s \rightleftarrows Bs$	
*	$Bs \rightleftarrows cBS$ r_1	$r_1=[k_1\cdot k_B\cdot(P_B-P_{cB}/K_{e1})/D]$
*	$cBs \rightleftarrows tBs$ r_2	$r_2=[k_2\cdot K_{cB}\cdot(P_{cB}-P_{tB}/K_{e2})/D]$
*	$Bs \rightleftarrows tBs$ r_3	$r_3=[k_3\cdot K_B\cdot(P_B-P_{tB}/K_{e3})/D]$
	$cBs \rightleftarrows cB+s$	$D=[1+K_B\cdot P_B+K_{cB}\cdot P_{cB}+K_{tB}\cdot P_{tB}]$
	$tBs \rightleftarrows tB+s$	
	Model I-2	
	$B+2s \rightleftarrows 2B_{1/2}s$	
*	$2B_{1/2}s \rightleftarrows cBs+s$ r_1	$r_1=[k_1\cdot K_B\cdot(P_B-P_{cB}/K_{e1})/D]$
*	$cBs \rightleftarrows tBs$ r_2	$r_2=[k_2\cdot K_{cB}\cdot(P_{cB}-P_{tB}/K_{e2})/D]$
*	$2B_{1/2}s \rightleftarrows tBs+s$ r_3	$r_3=[k_3\cdot K_B\cdot(P_B-P_{tB}/K_{e3})/D]$
	$cBs \rightleftarrows cB+s$	$D=[(1+\sqrt{K_B\cdot P_B}+K_{cB}\cdot P_{cB}+K_{tB}\cdot P_{tB})^2]$
	$tBs \rightleftarrows tB+s$	
	Model I-3	
	$B+2s \rightleftarrows 2B_{1/2}s$	
*	$2B_{1/2}s \rightleftarrows 2cB_{1/2}s$ r_1	$r_1=[k_1\cdot K_B\cdot(P_B-P_{cB}/K_{e1})/D]$
*	$2cB_{1/2}s \rightleftarrows 2tB_{1/2}s$ r_2	$r_2=[k_2\cdot K_{cB}\cdot(P_{cB}-P_{tB}/K_{e2})/D]$
*	$2B_{1/2}s \rightleftarrows 2tB_{1/2}s$ r_3	$r_3=[k_3\cdot K_B\cdot(P_B-P_{tB}/K_{e3})/D]$
	$2cB_{1/2}s \rightleftarrows cB+2s$	$D=[(1+\sqrt{K_B\cdot P_B}+\sqrt{K_{cB}\cdot P_{cB}}+\sqrt{K_{tB}\cdot P_{tB}})^2]$
	$2tBs_{1/2} \rightleftarrows tB+2s$	
	Model I-4	
	$B+s \rightleftarrows Bs$	
*	$Bs+s \rightleftarrows 2cB_{1/2}s$ r_1	$r_1=[k_1\cdot K_B\cdot(P_B-P_{cB}/K_{e1})/D]$
*	$2cB_{1/2}s \rightleftarrows 2tB_{1/2}s$ r_2	$r_2=[k_2\cdot K_{cB}\cdot(P_{cB}-P_{tB}/K_{e2})/D]$
*	$Bs+s \rightleftarrows 2tB_{1/2}s$ r_3	$r_3=[k_3\cdot K_B\cdot(P_B-P_{tB}/K_{e3})/D]$
	$2cB_{1/2}s \rightleftarrows cB+2s$	$D=[(1+K_B\cdot P_B+\sqrt{K_{cB}\cdot P_{cB}}+\sqrt{K_{tB}\cdot P_{tB}})^2]$
	$2tBs_{1/2} \rightleftarrows tB+2s$	

• R_k ($k=B$, cB, tB) at different times for each isomer has been calculated according to Eq. 28.

• R_{ko}, for $\alpha=1$, has been obtained by using Eq. 2, calculating the values of r_{io} ($i=1$, 2, 3) at the same composition and temperature that R_k was calculated. Since the discrimination among the four models in Table 7 has not been concluded, R_{ko} values have been calculated taking into account each one of the four mentioned models in the r_{io} calculation. The values obtained for the ratio R_k/R_{ko} (for $k=B$, cB, tB) were very similar for all the four models I-1 to I-4.

As can be seen in Figure 7, the activity for the different reactions is the same. In this way, the experimental results support assuming the same number of active sites taking part in the controlling step (surface reaction in this case).

As a consequence of the above mentioned fact, and according to the coke precursor formation mechanism proposed

Table 8. Deactivation Kinetic Parameters of Nonlinear Multiresponse Regression from Activity-Time Data with Temperature as Variable

Model		h	n	m_{1B}	m_{2B}	m	$Ln\ kd_{Bo}$ Opt.	$Ln\ kd_{Bo}$ Max.	$Ln\ kd_{Bo}$ Min.	Ed_B/R Opt.	Ed_B/R Max.	Ed_B/R Min.	$Ln\ kd_{2Bo}$ Opt.	$Ln\ kd_{2Bo}$ Max.	$Ln\ kd_{2Bo}$ Min.	Ed_{2B}/R Opt.	Ed_{2B}/R Max.	Ed_{2B}/R Min.	SRC·10^5
D-1	I-1	1	1	1	1	1	0.299	3.59	0.239	2,120	2,760	1,490	10.3	12.2	8.32	6,650	7,610	5,690	2.87
D-2	I-2	2	1	2	1	2	6.6	7.39	5.81	3,510	3,910	3,120	12.2	14.2	10.1	5,590	6,600	4,590	2.57
D-3	I-2	2	2	2	1	2	5.94	6.7	5.18	2,910	3,290	2,520	12.1	14.3	9.9	4,750	5,830	3,670	3.37
D-4	I-2	3	2	2	1	2	11.4	12.1	10.6	4,390	4,780	4,010	18.1	20.5	15.8	6,930	8,090	5,770	3.39
D-5	I-2	2	1	2	2	2	5.79	6.86	4.73	3,010	3,540	2,480	9.84	11.8	7.87	4,910	5,880	3,940	2.59
D-6	I-3	2	2	2	2	2	6.29	7.1	5.47	2,950	3,360	2,540	7.41	9.29	5.53	2,860	3,780	1,940	2.88
D-7	I-3	1	2	1	2	2	2.4	3.47	1.33	2,490	3,030	1,960	7.11	9	5.22	4,120	5,060	3,190	3.27
D-8	I-4	2	1	1	2	2	11	11.9	9.99	5,300	5,790	4,820	9.87	11.4	8.3	4,930	5,700	4,150	2.35
D-9	I-4	3	1	1	2	2	19.9	20.8	19	8,030	8,490	7,580	12.2	13.9	10.5	4,660	5,510	3,820	3.08

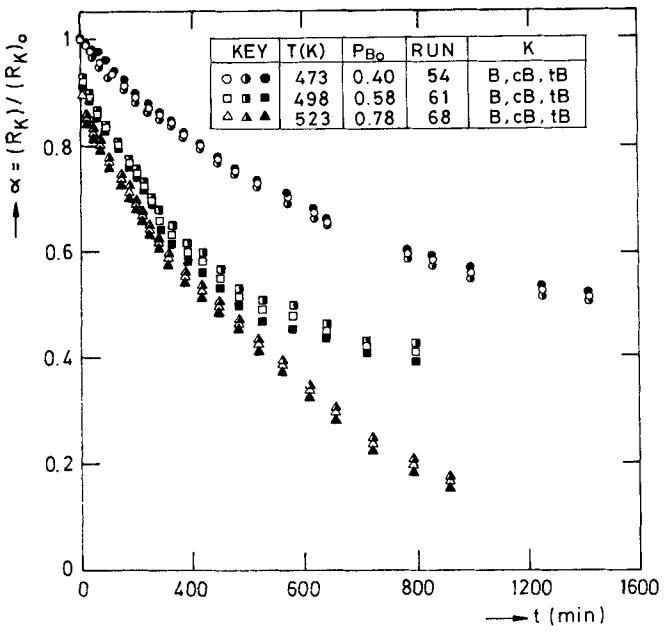

Figure 7. Activity decay calculated from butenes production rates.

by Eq. 7, the deactivation kinetic model can be written, as shown in Eq. 12. The values of the parameters m_{1B}, m_{2B}, h, and n appearing in such an equation depend on both the adsorption mechanism assumed for the main reaction and the coke precursor formation mechanism. The values of m_{1B} and m_{2B} can be deduced for the four models given by Table 7. The values of h and n considered have been 1, 2, and 3 for h and 0, 1, and 2 for n. Therefore, according to Eq. 12, combining the four possible values of m_{1B} and m_{2B} with the three values of each one for h and n, 36 different models are obtained.

The experimental data of the runs of Group III enable calculation of P_B, P_{cB}, P_{tB}, and α at different time values. These data have been analyzed taking into account the 36 mentioned models, obtaining the values of $-d\alpha/dt$ by fitting α values to a potential-exponential function of time for each run (García-Ochoa et al., 1992). In all the cases, the valúes of adsorption equilibrium constants, K_B and K_{2B} have been fixed at the values previously calculated in the determination of the kinetic model of the main reaction. Only the kinetic deactivation parameters, kd_B and kd_{2B}, have been permitted to float. In this way, their optimum values have been calculated for each model by nonlinear multiresponse regression (Marquardt, 1963). This calculation was carried out in two steps:

- In the first step the optimization was made at each temperature. At this step, six of the 36 models were rejected because of the negative value of some parameter at some temperature, and another 15 models were rejected because an anomalous variation with temperature was found of some of the parametes, kd_B and kd_{2B}.
- The 15 remaining models were subjected to nonlinear regression with the temperature as a variable, assuming an exponential of Arrhenius type of both kd_B and kd_{2B} with temperature. Six models were rejected at this step, because a great residual sum was found. Table 8 shows the parameter values obtained for the nine models remaining at this step together with their confidence intervals (for 95%) and the m_{1B}, m_{2B}, h, and n values employed with each model. Also, the mechanism of the main reaction corresponding to each one of these models (from Table 7), together with the m value for each mechanism is given in Table 8.

With the data analyzed until this moment it is not possible the final discrimination among the nine models considered in Table 8. To complete this discrimination the coke production rate data must be taken into account.

Kinetic Model for Coke Deposition

The kinetic equation of coke production is given by Eq. 5. The relationship with deactivation rate, Eq. 12, can be established if catalyst activities of both the main reaction, α, and the coke formation reaction, α_c, are achieved. From the experimental results given in Table 4, obtained by analysis of catalyst samples recovered from the BSTR, it can be seen when α has decreased to a value of 0.3, the coke content has hardly increased to 1% (w/w). No changes in physical properties, such as internal surface area and pore volume, is found for such low coke content. Therefore, it can be assumed that coke is formed in a monolayer, and the deactivation is due to active site coverage. In this case, a linear relationship as shown in Eq. 15 between coke and precursor can be assumed, the latter being formed according to the mechanism described by Eq. 7. Also, in this case, the relationship between α and α_c can be given by Eq. 18, and the relationship between α and C_c can be given by Eq. 16. Therefore, the coke production rate is given by Eq. 17. The results in Table 4 also show that the coke composition (C and H by elemental analysis) can be considered almost constant. With this last assumption, the experimental data given by Group IV of experiments obtained in electrobalance can be interpreted according to Eqs. 22 or 23, depending on the h value; in these equations the function $\psi(T, P)$ must be the same as that in Eqs. 4 and 12. On the other hand, in the runs carried out in the electrobalance the 1-butene conversion is so small that it can be assumed that the 2-butene partial pressures are zero (P_{cB}, $P_{tB} \rightarrow 0$); then Eq. 12 can be simplified yielding:

$$\psi = \frac{kd_B \cdot K_B^{h/m_{1B}} \cdot P_B^{(h/m_{1B})+n}}{(1 + K_B \cdot P_B^{1/m_{1B}})^h} \tag{30}$$

The data C_c vs. t collected in Group IV of experiments can be interpreted according to these assumptions, taking into account the nine models not rejected yet, considered in Table 8. Therefore, experimental data has been fitted by nonlinear regression (Marquardt, 1963) to Eqs. 22 or 23 and Eq. 30 with temperature as variable obtaining the results given in Table 9. Three parameters were let to float: kd_{Bo}, Ed_B/R (corresponding to the function of kd_B with temperature) and the ratio $S_o \cdot Mc/h$. While the value of K_B, was previously calculated in the determination of the kinetic model of the main reaction, the parameter value depends on the kinetic model considered (Table 7).

Discussion: Final Model Selected

By comparing the results in Tables 8 and 9, it can be seen that the values calculated for Ed_B/R from both types of data, α vs. t and C_c vs. t, are quite different for most of the models. They have similar values for only one model with reference

Table 9. Deactivation Kinetic Parameters of Coke-Time Data, Using Eq. 22 or 23 with $\psi(T, P)$ Following Eq. 30 Kinetic Model

	$S_o \cdot M_c/h \times 10^2$ (g Coke/g Cat)			$Ln\ k_{dBo}$			E_{dB}/R (K)			
Model	Opt.	Max.	Min.	Opt.	Max.	Min.	Opt.	Max.	Min.	SRC
D-1	1.30	1.33	1.26	9.75	10.77	8.73	7,071	7,567	6,574	14.6
D-2	1.55	1.60	1.50	15.29	16.41	14.17	7,855	8,389	7,320	11.1
D-3	1.35	1.39	1.30	15.17	16.88	13.46	7,354	8,179	6,528	19.3
D-4	1.70	1.76	1.63	15.63	17.04	14.21	7,959	8,634	7,283	13.6
D-5	1.55	1.60	1.49	15.53	16.65	14.42	7,867	8,403	7,331	11.0
D-6	1.34	1.39	1.30	15.42	17.13	13.71	7,370	8,198	6,542	21.4
D-7	1.19	1.23	1.15	10.93	12.44	9.42	6,576	7,315	5,836	27.5
D-8	1.36	1.40	1.30	12.46	14.15	10.77	7,499	8,316	6,681	21.4
D-9	1.36	1.41	1.30	14.56	16.18	12.95	8,168	9,031	7,305	13.5

D-9. This model has been finally selected as the most adequate to describe coke deposition rate; therefore, the corresponding kinetic model is selected for both deactivation rate and main reaction. Such a model corresponds to mechanism I-4 in Table 7, being $h = 3$ and $n = 1$. That is, three adsorbed molecules (of any butene, reactant, or product) are reacting to one molecule in gas-phase yielding the coke precursor, and $m = 2$. Two active sites are thus involved in the rate controlling step of the surface reaction. The final model selected is given by Eq. 31. Figure 8 is an example of fitting of the values given by this model to the experimental data achieved in BSTR of 1-butene, 2-cis butene, and 2-trans-butene conversions at different times in

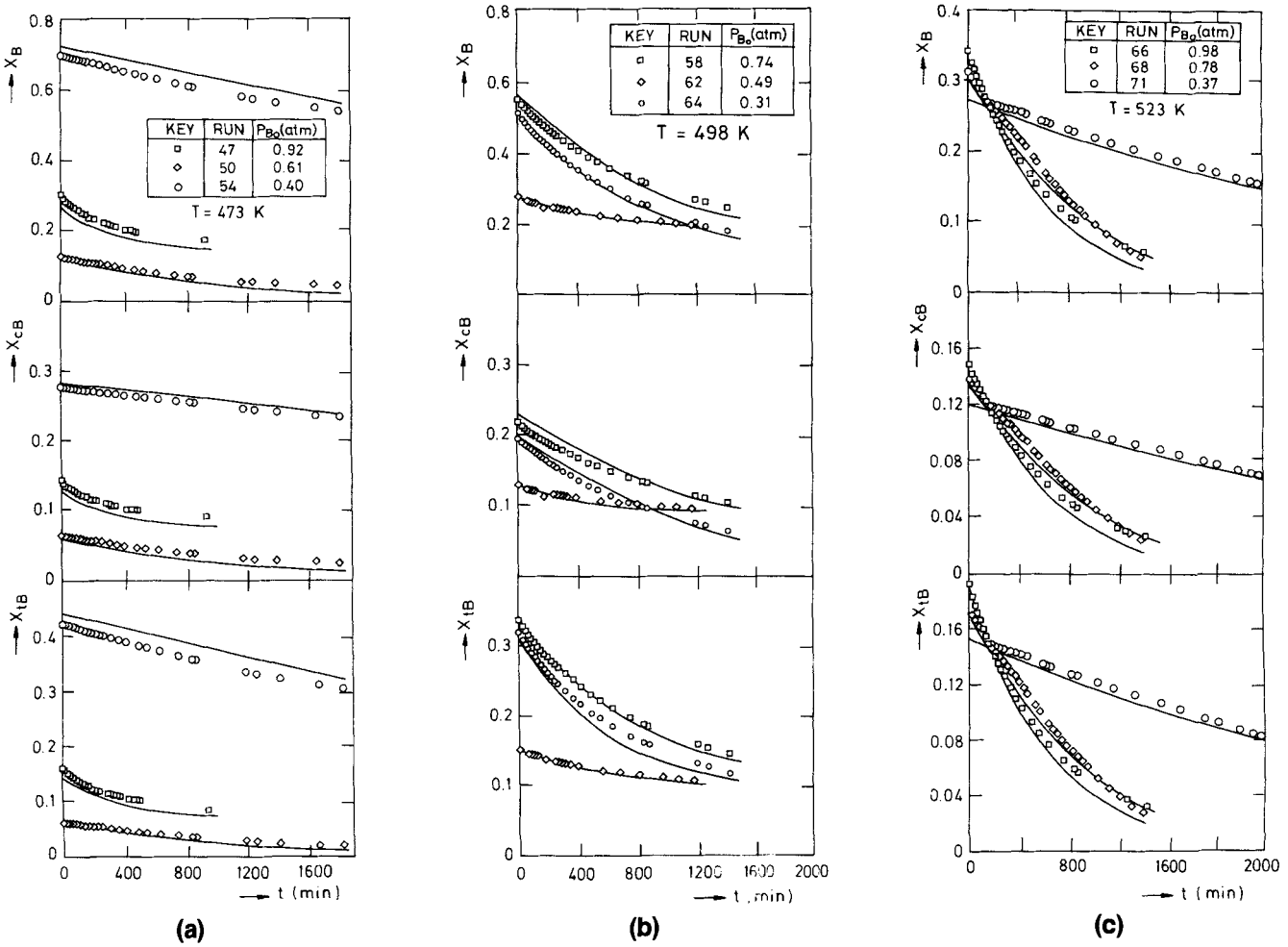

Figure 8. Calculated vs. experimental 1-butene conversion at different times for runs in BSTR as integral reactor, employing Eq. 31.

(a) 473 K; (b) 498 K; (c) 523 K.

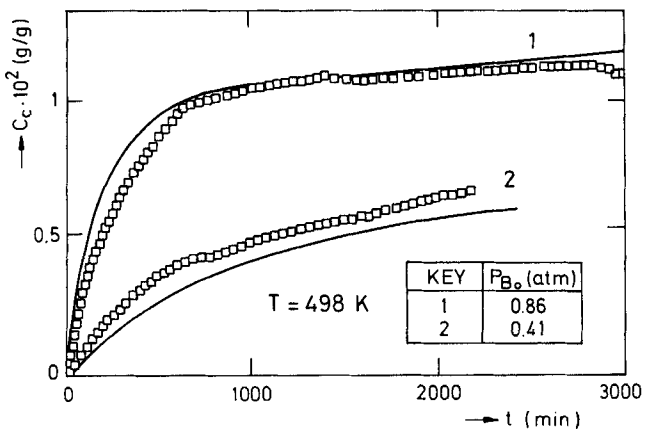

Figure 9. Calculated vs. experimental coke content at different times for runs in electro-balance with Eqs. 23 and Eq. 30 for model D-9 of Table 10.

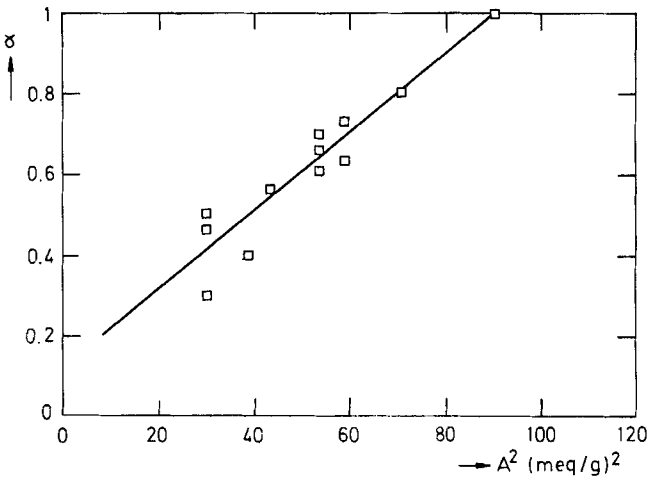

Figure 11. Dependence of catalyst activity with catalyst acidity as a function A^2.

runs carried out at different operational conditions. Figure 9 is an example of the fitting of experimental results obtained in electrobalance.

In the model selected for 1-butene isomerization (Eq. 31) the number of active sites involved in the controlling step of the reaction rate, m, takes a value of 2. This value has been employed for fitting coke-activity data from Table 4 according to Eq. 16, as shown in Figure 10, obtaining the relationship of Eq. 32.

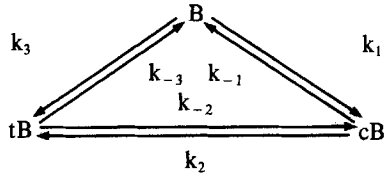

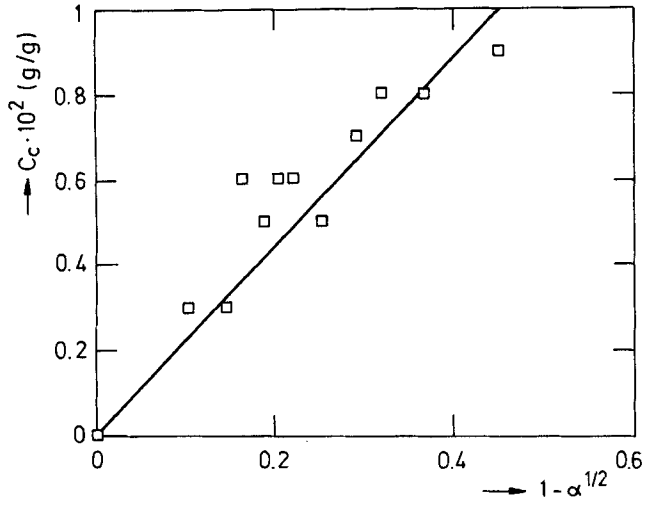

Figure 10. Dependence of catalyst coke content with catalyst activity as a function $(1-\alpha^{1/2})$.

$$r_1 = \frac{k_1 \cdot K_B \cdot \left(P_B - \frac{P_{cB}}{K_{e_1}}\right)}{D} \cdot \alpha$$

$$r_2 = \frac{k_2 \cdot K_{2B} \cdot \left(P_{cB} - \frac{P_{tB}}{K_{e_2}}\right)}{D} \cdot \alpha$$

$$r_3 = \frac{k_3 \cdot K_B \cdot \left(P_B - \frac{P_{tB}}{K_{e_3}}\right)}{D} \cdot \alpha$$

$$\alpha = \frac{1}{1 + \int_o^t \frac{kd_B \cdot K_B^3 \cdot P_B^4 + kd_{2B} \cdot K_{2B}^{3/2} \cdot (P_{cB}^{5/2} + P_{tB}^{5/2})}{[1 + K_B \cdot P_B + K_{2B}^{1/2} \cdot (P_{cB}^{1/2} + P_{tB}^{1/2})]^3} \cdot dt} \tag{31}$$

where:

$$\begin{aligned}
D &= [1 + K_B \cdot P_B + \sqrt{K_{2B}} \cdot (\sqrt{P_{cB}} + \sqrt{P_{tB}})]^2 \\
k_1 &= \exp(10.89 - 5{,}026/T) \text{ mol/(g·h)} \\
k_2 &= \exp(15.76 - 7{,}015/T) \text{ mol/(g·h)} \\
k_3 &= \exp(12.41 - 5{,}742/T) \text{ mol/(g·h)} \\
K_B &= \exp(-8.243 + 2{,}810/T) \text{ atm}^{-1} \\
K_{2B} &= \exp(-9.92 + 3{,}160/T) \text{ atm}^{-1} \\
kd_B &= \exp(19.9 - 8.030/T) \text{ min}^{-1} \cdot \text{atm}^{-1} \\
kd_{2B} &= \exp(12.2 - 4.660/T) \text{ min}^{-1} \cdot \text{atm}^{-1} \\
C_c &= 1.957 \times 10^{-2} \cdot (1 - \alpha^{1/2}) \text{ (g/g)}
\end{aligned} \tag{32}$$

Considering that catalyst acidity can be expressed as:

$$A = b_1 \cdot (S_o - S_p) \tag{33}$$

Taking into account Eq. 8, activity-acidity relationship can be written as:

$$\alpha = b_2 \cdot A^2 \tag{34}$$

The value of $m = 2$ is suitable to fit adequately the experimental data of acidity and activity from Table 4, as shown in Figure 11, being the relationship obtained:

$$\alpha = 0.0091 \cdot A^2 \tag{35}$$

Conclusions

1-Butene isomerization on a silica-alumina catalyst, between 448 and 523 K, is a chemical reaction that takes place according to a reaction scheme in which 1-butene yields both 2-cis- and 2-trans-butene. Also, the interconversion reaction between both 2-butene isomers takes place; being another isomer, isobutene, is not obtained in a significant concentration in the experimental interval of the operational condition studied. Such a triangular reaction scheme is confirmed by the value of initial selectivity to 2-cis-butene, S_c, close to 1 at all the temperatures studied. This also indicates that only one surface intermediate is able to evolve yielding both 2-cis-butene or 2-trans-butene. This surface intermediate has been proposed to be a secondary butyl carbenium ion (Hightower and Hall, 1967). The value of S_c close to 1 has also been found by other authors (Hightower and Hall, 1967; Vinek et al., 1985; Aguayo et al., 1990).

Analyzing the data of conversion-time obtained in a BSTR for fresh catalyst, it can be concluded that surface reaction is the controlling step of the rate process. Four different mechanisms given in Table 7 can be considered as yielding kinetic models able to fit such experimental results in a wide interval of experimental conditions including temperatures between 448 and 523 K and feed composition, P_{Bo}, between 0.20 and 1.02 atm. This is with similar values of the fitting parameters and activation energy for the kinetic parameter around 12,000 cal/mol, in agreement with the one found by Hightower and Hall (1967).

Assuming a mechanism for coke formation, taking into account a number of adsorbed molecules, h, reacting with a number of molecules in the gas phase, n, to yield a coke precursor, several kinetic models can be proposed for both deactivation rate (r_d) and for coke deposition rate (r_c), depending on the kinetic model of the main reaction and the h and n values. From the interpretation of both data, those of conversion time obtained in BSTR, and those of coke content time from an electrobalance, only one of the models considered yields similar parameter values in the deactivation rate and in the coke formation rate equations. For the coke deposition rate determination, it must be assumed that the coke is formed in a monolayer and the catalyst deactivation is carried out by active site coverage. This is reasonable, taking into account that the maximum coke content achieved was around 1% (w/w) while the catalyst activity decreased to 0.3. The value of the activation energy of the deactivation kinetic parameter, kd, was the one chosen for comparison between both types of data (activity time and coke content time) and interpretation methods.

Therefore, a kinetic model for the main reaction rate, making up a triangular reaction scheme and kinetic equations for each of the three reactions involved, can be selected. Such kinetic equations correspond to a mechanism according to which the same number of active sites take part in all the three reactions. This number, m, is equal to 2. In this case, the catalyst activity for the three reactions must be the same, as confirmed by experimental results; moreover, the value $m=2$ permits us to establish two relationships between catalyst activity and coke content and between catalyst activity and acidity. This is experimentally found to be given by Eqs. 32 and 35. The deactivation by active site coverage due to coke deposited in a monolayer is also in agreement with the nonvariation of physical properties of the catalyst, such as surface and pore volume, found for different coke content and activity of the catalyst.

The coke precursor is formed according to a mechanism which considers that three adsorbed molecules of butene isomers ($h=3$) react with one molecule in the gas phase ($n=1$). With these assumptions, a kinetic model for the main reaction, the deactivation rate and the coke deposition rate given by Eq. 31 can be proposed which fits all the experimental data obtained (conversion-time and coke content-time) in a wide interval of temperature (448–523 K) and composition (1.02–0.10 atm of 1-butene partial pressure), yielding a very good fitting as shown in Figures 8 and 9.

Acknowledgment

This work has been supported by D.G.I.C.Y.T. under contract no. PB89-0118, and the infrastructure support GR88-0129. The authors wish also to thank Research Centers of CEPSA and REPSOL for some of the measurements of the catalyst.

Notation

A = catalyst acidity (meq. n-butilamine/g)
$b_{1,2}$ = parameter in Eqs. 33 and 34
B = 1-butene
C_c = total catalyst coke content (g coke/g catalyst)
C_{cm} = catalyst coke content in monolayer (g coke/g catalyst)
C_{Psh} = coke precursor concentration (mol coke/g catalyst)
d = order of activity term in deactivation rate equation, Eq. 4
E = activation energy (cal/mol)
F_i = molar flow of component i (mol/h)
ΔH = enthalpy increment (cal/mol)
k = kinetic constant (mol/g·h)
k_o = preexponential of kinetic constant (mol/g·h)
K = adsorption constant (atm^{-1})
K_e = equilibrium constant ($K_{ei}=k_i/k_{-i}$, $i=1, 2, 3$)
K_o = preexponential factor of adsorption constant (atm^{-1})
kd = deactivation kinetic constant in Eq. 12 ($min^{-1}\cdot atm^{-1}$)
kd' = deactivation kinetic constant, Eq. 11 ($mol\cdot min^{-1}\cdot atm^{-1}\cdot g^{-1}$)
m = number of active sites taking part in the controlling step on main reaction (surface reaction in this case)
M_c = average coke molecular weight ($g\cdot mol^{-1}$)
P = pressure (atm)
P_i = partial pressure of component i (atm)
P_T = total pressure (atm)
r = reaction rate ($mol\cdot g^{-1}\cdot h^{-1}$)
r_c = coke production rate (g coke·g $cat^{-1}\cdot min^{-1}$)
r_d = deactivation rate (min^{-1})
r_o = fresh catalyst reaction rate ($mol\cdot g^{-1}\cdot h^{-1}$)
R = gas constant ($cal\cdot mol^{-1}\cdot K^{-1}$), production rate ($mol\cdot g^{-1}\cdot h^{-1}$)
s = active site
S_o = active site concentration in fresh catalyst (mol/g)
S_g = specific surface (m^2/g)
t = time (min)
T = temperature (K)
V_p = pore volume (cm^3/g)
W = catalyst weight (g, mg)
W/F = space time ($g\cdot s/mol$)
X = conversion
Y = molar fraction in gas phase

Greek letters

α = activity for isomerization reactions
ϕ = coke function in Eq. 6
φ = deactivation function (g coke·g $cat^{-1}\cdot min^{-1}$) in Eq. 5
ψ = deactivation function (min^{-1}) in Eq. 4

Literature Cited

Acharya, D. R., A. J. Allen, and R. Hughes, "A Small-Angle Neutron Scattering Investigation of Coke Deposits on Catalysts," *Ind. Eng. Chem. Res.*, **29**, 1119 (1990).

Aguayo, A. T., J. M. Arandés, M. Olazar, and J. Bilbao, "Isomerization of Butenes as a Test Reaction for Measurements of Solid Catalyst Acidity," *Ind. Eng. Chem. Res.*, **29**, 1172 (1990).

Ballivet, D., D. Barthomeuf, and M. Y. Trambouze, "Etude de la Désactivation d'un Catalyseur Silice-Alumine: Mise en Evidence de Deux Types de Sites d'Activités Différentes," *C. R. Acad. Sc. Paris, Serie C*, **271**, 118 (1970).

Boudart, M., D. E. Mears, and M. A. Vannice, "Kinetics of Heterogeneous Catalytic Reactions," *Ind. Chem. Belge*, **32**, 281 (1967).

Carrá, S., and V. Ragaini, "On the Mechanism of 1-Butene Isomerization on Supported Palladium," *J. Catal.*, **10**, 230 (1968).

Chang, C. C., W. C. Conner, and R. J. Kokes, "Butene Isomerization over Zinc Oxide and Chromia," *J. of Phys. Chem.*, **77**, 1957 (1973).

Chu, C., "Effect of Adsorption on the Fouling of Catalyst Pellets," *Ind. Eng. Chem. Fundam.*, **7**, 509 (1968).

DePaw, R. P., and G. F. Froment, "Deactivation of a Platinum Reforming Catalyst in a Tubular Reactor," *Chem. Eng. Sci.*, **30**, 789 (1975).

Dumez, F. J., and G. F. Froment, "Dehydrogenation of 1-Butene into Butadiene. Kinetics, Catalyst and Reactor Design," *Ind. Eng. Chem. Process Des. Dev.*, **15**, 291 (1976).

Eliyas, A., L. Petrov, Ch. Vladov, and D. Shopov, "Kinetics of Isomerization of Butenes over an Industrial CoO-MoO_3/Al_2O_3 Catalyst: II. Kinetic Model Construction," *Appl. Catal.*, **33**, 295 (1987).

Foster, N. F., and R. J. Cvetanovic, "Stereoselective Catalytic Isomerization of *n*-Butenes," *J. Am. Chem. Soc.*, **82**, 4274 (1960).

Froment, G. F., and K. B. Bischoff, *Chemical Reactor Analysis and Design*, 2nd ed., Wiley, New York (1990).

García-Ochoa, F., A. Romero, and J. Querol, "Modeling of Thermal Octane Oxidation in Liquid Phase," *Ind. Eng. Chem. Res.*, **28**, 43 (1989).

García-Ochoa, F., J. Querol, and A. Romero, "Modeling of the Liquid Phase *n*-Octane Oxidation Catalyzed by Cobalt," *Ind. Eng. Chem. Res.*, **29**, 1989 (1990).

García-Ochoa, F., A. Romero, and V. Santos, "Comparison of Methods for Determining the Kinetic Parameters in Complex Reactions," *Int. Chem. Eng.*, **32**, 538 (1992).

Ghorbel, A. G., C. Hoan-Van, and S. J. Teichner, "Catalytic Activity of Amorphous Alumina Prepared in Aqueous Media: II. Nature of Active Sites in the Isomerization of Butene-1," *J. Catal.*, **33**, 123 (1974).

Goldwasser, J., J. Engelhardt, and W. K. Hall, "The Isomerization and Metathesis of *n*-Butenes: I. Unreduced Molybdeno-Alumina Catalysts," *J. Catal.*, **70**, 275 (1981).

Haag, W. O., and H. Pines, "The Kinetic of Carbanion-Catalyzed Isomerization of Butenes and 1-Pentene," *J. Am. Chem. Soc.*, **82**, 387 (1960a).

Haag, W. O., and H. Pines, "Alumina: Catalyst and Support: III. The Kinetics and Mechanisms of Olefin Isomerization," *J. Am. Chem. Soc.*, **82**, 2488 (1960b).

Hightower, J. W., and W. K. Hall, "Tracer Studies of Acid-Catalyzed Reactions: V. Carbon -14 Kinetic Studies of *n*-Butene Isomerization over Alumina and Silica-Alumina Catalysts," *J. Phys. Chem.*, **71**, 1014 (1967).

Hightower, J., H. R. Gerberich, and W. K. Hall, "Tracer Studies of Acid-Catalyzed Reactions: VI. Rate Constants for *n*-Butene Interconversion Reactions over Alumina, Fuorided Alumina, and Silica-Alumina," *J. Catal.*, **7**, 57 (1967).

Hougen, O. A., K. M. Watson, and R. A. Ragatz, *Chemical Process Principles: II. Thermodynamics*, Wiley, New York (1954).

Jodra, L. G., A. Romero, and J. Corella, "Cinética y Mecanismo del Envenenamiento del Catalizador de Cobre/Amianto en la Deshidrogenación del Alcohol Bencílico en Fase Gaseosa," *An. Ouim. Ser. A.*, **72**, 823 (1976).

Levenspiel, O., "Experimental Search for a Simple Rate Equation to Describe Deactivating Porous Catalyst Particles," *J. Catal.*, **25**, 265 (1972).

Lin, Ch., S. W. Park, and J. Hatcher, Jr., "Zeolite Catalyst Deactivation bu Coking," *Ind. Eng. Chem. Process Des. Dev.*, **22**, 609 (1983).

Marquardt, F. W., "An Algorithm for Least-Squares Estimation of Nonlinear Parameters," *J. Soc. Ind. Appl. Math.*, **2**, 431 (1963).

Medema, J., "Isomerization of Butene over Alumina," *J. Catal.*, **37**, 91 (1975).

Nam, I. S., and J. R. Kitrell, "Use of Catalyst Content in Deactivation Modeling," *Ind. Eng. Chem. Process Des. Dev.*, **23**, 237 (1984).

Ragaini, V., and M. G. Cattania-Sabbadini, "Activity, Selectivity, and XPS Analysis of γ-Alumina-Supported Group VIII Metals Used in 1-Butene Isomerization in the Absence of Molecular Hydrogen," *J. Catal.*, **93**, 161 (1985).

Reid, R. C., J. M. Prausnitz, and T. K. Sherwood, *The Properties of Gases and Liquids*, 3rd ed., McGraw-Hill, New York (1977).

Rosynek, M. P., and J. S. Fox, "Characterization of Catalytic Lanthanum Oxide for Double Bond Isomerization of *n*-Butenes," *J. Catal.*, **49**, 285 (1977).

Santos, A., "Desactivación de Catalizadores por Coque," PhD Thesis, Universidad Complutense, Madrid (1992).

Vinek, H., J. A. Lercher, and H. Noller, "Acid-Base Properties of Silica-Alumina Oxides Derived from NaX Zeolites: III. Catalytic Activity in Dehydration of Alcohols and in Isomerization of But-1-ene," *J. Molec. Catal.*, **30**, 353 (1985).

Manuscript received Feb. 16, 1993, and revision received Feb. 8, 1994.